



ORIGINAL ARTICLE

Kinetics and mechanism of incorporation of zinc(II) into tetrakis(1-methylpyridium-4-yl)porphyrin in aqueous solution

Ahsan Habib ^{a,*}, Rokayea Islam ^a, Mrittika Chakraborty ^a, Salma Serniabad ^{a,b},
Mohammad Shamim Khan ^a, Deepro Sanjid Qais ^a, Md Emran Quayum ^a,
Md Ashraf Alam ^b, Iqbal Mohammad Ibrahim Ismail ^c, Masaaki Tabata ^d

^a Department of Chemistry, Faculty of Science, University of Dhaka, Dhaka 1000, Bangladesh

^b Department of Applied Chemistry and Chemical Engineering, Noakhali Science and Technology University, Noakhali 3814, Bangladesh

^c The Center of Excellence in Environmental Studies & Department of Chemistry, King Abdulaziz University, Jeddah 21589, Saudi Arabia

^d Department of Chemistry, Faculty of Science and Engineering, Saga University, 1, Honjo-machi, Saga 840-8502, Japan

Received 2 April 2020; accepted 7 June 2020

Available online 19 June 2020

1. Introduction

The kinetics and mechanism of metal ion incorporation into the porphyrin core have been the subject of extensive study due to their widespread occurrence and significant role in biological and artificial photosynthetic systems. For instance, in the biosynthesis of heme, the protoporphyrin IX ring is synthesized and iron(II) is subsequently incorporated into the porphyrin core. Kinetic studies of metalloporphyrin formation provide the mechanistic pathways of the relevant reactions. Proper mechanisms are expected in developing new drugs that enhance or inhibit certain biochemical reactions through metalation or dematallation of porphyrins in the biological systems. Hambright and Chock (1974) proposed the general

mechanism for the metalation of porphyrins for the first time and was reviewed by other groups (Hambright, 1975; Lavallee, 1985; Tanaka, 1983; Tabata and Tanaka, 1991; Habib et al., 2004). However, the overall mechanism is relatively complex, since the rate of formation of the metalloporphyrin is several orders of magnitude lower than that of the complex formation of open-chain ligands (Margerum and Cayley, 1978). In order to accelerate the metalation, several methods have been proposed, especially from the analytical points of view (Shamim and Hambright, 1980): (i) the use of substitution reactions of cadmium(II) or mercury(II)porphyrins (Tabata and Tanaka, 1983; Funahashi et al., 1986), (ii) the use of porphyrins with substituents at the pyrrole nitrogen (Lavellee, 1987; Kawamura et al., 1988), (iii) the use of reducing agents such as hydroxylamine, ascorbic acid etc. (Thompson and Krishnamurthy, 1979; Sutter and Hambright, 1993), (iv) the introduction of functional groups to bind metal ions in the vicinity of the porphyrin nucleus (e.g., tetracarboxylic acid “pocket-fence” porphyrins) (Tabata and Ishimi, 1997) and (v) carry out reactions at a suitable solution pH where hydroxo ligands coordinated to the metal ions (Hambright and Chock, 1974; Tanaka, 1983;

* Corresponding author.

E-mail address: habibchem@du.ac.bd (A. Habib).

Peer review under responsibility of King Saud University.



Production and hosting by Elsevier

Habib et al., 2004). Any one of the above mentioned methods can enhance the reactivity of the relevant metal ion towards the free base porphyrin. For example, the enhanced reactivity for type (v) is ascribed to the formation of hydrogen bonding between the oxygen atom of the hydroxo ligand and the pyrrolic hydrogen atom of the free base porphyrin (Hambright and Chock, 1974; Tanaka, 1983; Habib et al., 2004).

Multifunctional properties of porphyrins and metalloporphyrins have already been attracted by many research groups worldwide to extend the porphyrin research in various fields. Metalation and/or demetalation of porphyrins provide proper mechanistic pathways of the relevant reaction thus much attention has been paid on investigation of the kinetics and mechanism of formation of the metalloporphyrins of many metals such as, transition metals, alkali and alkaline earth metals etc. (Hambright, P., 1975; Longo et al., 1979; Tanaka, 1983; Lavallee, 1985; Habib et al., 2004). Kinetics of formation of Zn(II)porphyrins have also been studied by some research groups (Hambright and Chock, 1974; Paquette and Zador, 1978; Thompson and Krishnamurthy, 1979; Sutter and Hambright, 1993; Tabata and Ishimi, 1997), however, so far least attention has been focused on speciation of Zn^{2+} ion which is an indispensable step to ascertain the mechanism of the desired reaction.

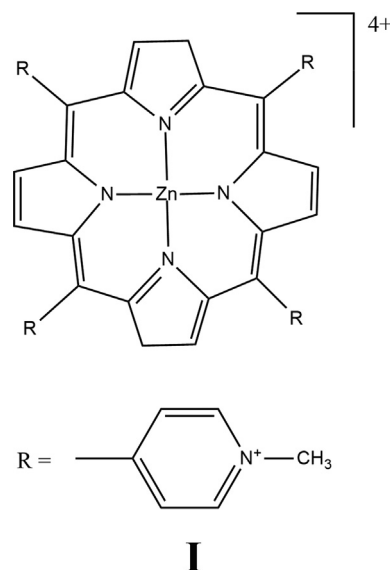
Zinc is an essential element for terrestrial life since it is required as either a structural component or reaction site in numerous proteins, the zinc-binding portions of which are highly conserved among species (Roohani et al., 2013). In spite of the important use of the porphyrins as hemoglobin or chlorophyll, now-a-days their use in the treatment of African trypanosomiasis, psoriasis, atheromatous plaque, several viral and bacterial infections including AIDS, as photodynamic therapeutic (PDT) agent in cancer has become undoubtedly porphyrins' most pertinent applications (Nyarko et al., 2004a; Rapozzi et al., 2014; Varchi et al., 2015; Imran et al., 2018; Ptaszynska et al., 2018; Tsolekile et al., 2019).

The medicinal importance of zinc and porphyrins in biological system motivated to study the kinetics and mechanism of the incorporation of Zn^{2+} into the free base porphyrin, tetrakis(1-methylpyridium-4-yl)porphyrin (H_2TMPyP^{4+}). In this paper, speciation of Zn^{2+} in aqueous system as a function of solution pH has studied at 25 ± 1 °C and applied the speciation knowledge along with the means of a speciation diagram developed by Choi et al. (2013), to study the kinetics of the formation of $ZnTMPyP^{4+}$ complex, I (Scheme 1) to ascertain proper mechanistic pathway of the metalation reaction.

2. Experimental

2.1. Reagents and materials

5,10,15,20-tetrakis(1-methylpyridinium-4-yl)porphyrin, $[H_2TMPyP]^{4+}$, was purchased as a tosylate from Dojindo Chemical Institute, Kumamoto, Japan. The porphyrin solution was prepared by dissolving 68.18 mg of $[H_2TMPyP]^{4+}$ tetratosylate in 50 mL of distilled water. The standardization of the porphyrin solution was done by spectrophotometric titration (molar ratio method) with a standard copper(II) solution (Makino and Itoh, 1981; Nyarko et al., 2004b; Habib et al., 2004). Zinc solutions were prepared by dissolving $ZnCl_2$ in aqueous solution and their concentrations were determined



Scheme 1 Tetracation zinc(II) porphyrin, $[Zn(TMPyP)]^{4+}$, I.

by atomic absorption spectrophotometry (Perkin Elmer, AAAnalyst 200). Sodium chloride, sodium nitrate, sodium hydroxide and hydrochloric acid were purchased from Merck, Germany, used as obtained without further purification. Tetracation zinc(II) porphyrin, $[ZnTMPyP]^{4+}$, was prepared and absorption spectra were recorded in water at pH 10.30 containing 0.1 M $NaNO_3$. Absorption maximum (λ_{max}) and molar extinction coefficient (ϵ) of the prepared $[ZnTMPyP]^{4+}$ complex were 437 nm and $181 \times 10^3 M^{-1}cm^{-1}$ respectively (Anula et al., 2006). Buffer solutions were prepared with acetic acid and sodium acetate. Distilled water was used throughout the experiment.

2.2. Speciation of Zn^{2+} complexes

A series of $Zn^{2+}_{(aq)}$ solutions of 5.00×10^{-3} M at various pH ranging from 2.28 to 11.30 in 50 mL volumetric flask were prepared separately. The ionic strength was adjusted to 0.10 M by adding $NaNO_3$. Either HCl or NaOH was used to adjust the solution pH in the acetate buffer ($[Acetate] = 0.02$ M). A double beam UV-vis spectrophotometer (SHIMADZU, Model UV-1800) was used to record the spectra of Zn^{2+} species in the wavelength range from 250 to 400 nm. A series of spectrophotometric titrations was carried out within a range of acetate buffer concentrations from 0 to 1.00×10^{-2} M with Zn^{2+} ion under the same experimental conditions. Results show that the acetate buffer has negligible complexing abilities with the Zn^{2+} species. The pH of the solutions was measured by using a pH meter (HANNA HI 2211).

2.3. Kinetics of Zn^{2+} incorporation into $[H_2TMPyP]^{4+}$

The kinetic runs were carried out under pseudo-first order condition within a pH range from 4.07 to 11.55 at a constant ionic strength, $I = 0.10$ M ($NaNO_3$). The concentrations of H_2TMPyP^{4+} was 1.24×10^{-5} M and Zn^{2+} was varied within a range from 0.25×10^{-3} to 5.00×10^{-3} M. The metalloporphyrin was prepared in a 1-cm cell compartment, maintained

at 25 ± 0.1 °C, by mixing the porphyrin solution with the Zn^{2+} solution. These solutions were pre-equilibrated at the reaction temperature. The change in the absorbance was recorded with time at 422 nm (λ_{max} of $[\text{H}_2\text{TMPyP}]^{4+}$) by using a double-beam UV-Vis spectrophotometer (SHIMADZU, Model UV-1800). Two isosbestic points, 430 and 480 nm, were found in the visible region as the porphyrin reacted with Zn^{2+} to form the $[\text{ZnTMPyP}]^{4+}$ complex I (Scheme 1). The spectral pattern of the formation of $[\text{ZnTMPyP}]^{4+}$ complex with time is shown in Fig. 1. The existence of the isosbestic points indicates that the free base porphyrin and the metalloporphyrin are the only absorbing species present. Plots of $\ln(A_t - A_\infty)$ vs time were linear over two to three half-lives and the slope of such plots yielded the observed rate constants (k_{obs}). Rate constants for the reactions were determined at different zinc concentrations, pH values and various ionic strengths. The duplicate runs under the same experimental conditions agreed within 5% error. The addition of acetate did not affect the spectra of the porphyrin. The pH of the solutions was measured by using a pH meter (Hanna HI 2211).

3. Results and discussion

3.1. Speciation of Zn^{2+}

In aqueous solution, Zn^{2+} ion predominantly exists as an octahedral hexaaqua complex ion, $[\text{Zn}(\text{H}_2\text{O})_6]^{2+}$, particularly in acidic pH (Burgess, 1978). However, aqueous solutions of zinc salts are mildly acidic because the aqua-ions take part in hydrolysis reaction with a $\text{p}K_a$ value about 9, thereby in formation of $[\text{Zn}(\text{H}_2\text{O})_5(\text{OH})]^{+}$ and H^{+} ions (Baes and Mesmer, 1976). Speciation diagram provides the presence of a specific reactive species at a particular solution pH that is required to establish a reaction mechanism through studying the kinet-

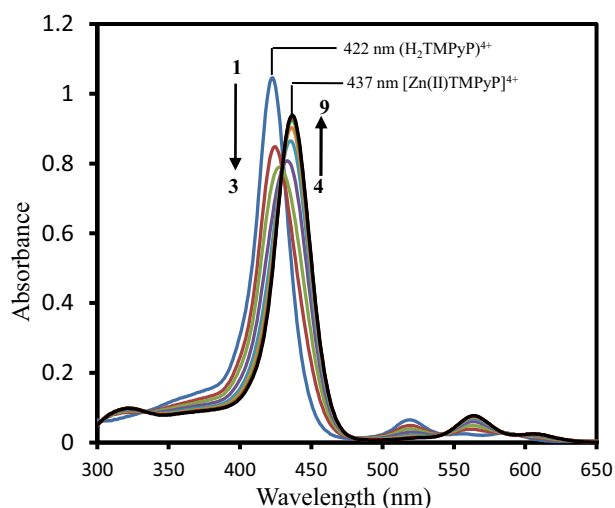


Fig. 1 Spectral pattern of formation of $\text{Zn}(\text{II})\text{TMPyP}^{4+}$ complex at 25 ± 1 °C. $I = 0.1$ M (NaNO_3). $[\text{Zn}^{2+}] = 1.00 \times 10^{-3}$ M; $[\text{H}_2\text{TMPyP}^{4+}] = 1.24 \times 10^{-5}$ M. Absorbance of $[\text{H}_2\text{TMPyP}^{4+}]$ ($\lambda_{\text{max}} = 422$ nm) decreases with time. The formation time are as follows: (1): 0; (2): 5; (3): 10; (4): 15; (5): 30; (6): 50; (7): 70; (8): 100 and (9): 140 min respectively.

ics of a particular reaction. A speciation diagram of Zn^{2+} -species with different solution pH has been constructed by Gallios and Vaclavikova (2008) using a visual MINTEQ program (Choi et al., 2013). The speciation diagram is shown in Fig. 2. As seen from the Fig. 2, aqua Zn^{2+} ($\text{Zn}_{(\text{aq})}^{2+}$) species is predominantly present within a pH range from 4 to 8.5, however, aqua-monohydroxo Zn^{2+} , $[\text{Zn}(\text{OH})_{(\text{aq})}^+]$, species exists with its maximum level at pH 8.5. The zinc-aqua-dihydroxo, $[\text{Zn}(\text{OH})_{2(\text{aq})}]$, species is mostly distributed within a pH range from 9.0 to 11.0 and its maximum level is observed at pH ~ 10.0 . With further increase the solution pH, zinc-trihydroxo, $[\text{Zn}(\text{OH})_3^-]$ and zinc-tetrahydroxo, $[\text{Zn}(\text{OH})_4^{2-}]$, species are formed and predominantly present at pH > 11.5 (Fig. 2).

The UV-Vis absorption spectra of zinc(II) chloride (1.0×10^{-3} M) with different solution pH are shown in the supplementary Fig. S-1. As seen from the supplementary Fig. S-1, the hexaaqua octahedral Zn^{2+} , $[\text{Zn}(\text{H}_2\text{O})_6]^{2+}$, ion exhibits a UV-Vis spectrum centered at $\lambda_{\text{max}} = 302$ nm at pH 2.28. With increasing the solution pH from 2.28 to 10.30, a slight hypochromicity without any red/blue shift is observed (supplementary Fig. S-1). This result suggests that the water molecules are strongly bound to the Zn^{2+} ion even at higher solution pH, 12.0 or 13.0 and successively displaced by the hydroxo (OH^-) ligand as a function of solution pH. Therefore, it may conclude that the hexaaqua Zn^{2+} species, $[\text{Zn}(\text{H}_2\text{O})_6]^{2+}$, co-exists with $[\text{Zn}(\text{H}_2\text{O})_{6-n}(\text{OH})_n]^{2-n}$ [$n = 1, \dots, 6$] in a pH range from 2 to 14 according to the following equations ($[\text{Zn}(\text{H}_2\text{O})_6]^{2+}$ is written as $\text{Zn}_{(\text{aq})}^{2+}$ for simplicity) (Choi et al., 2013):

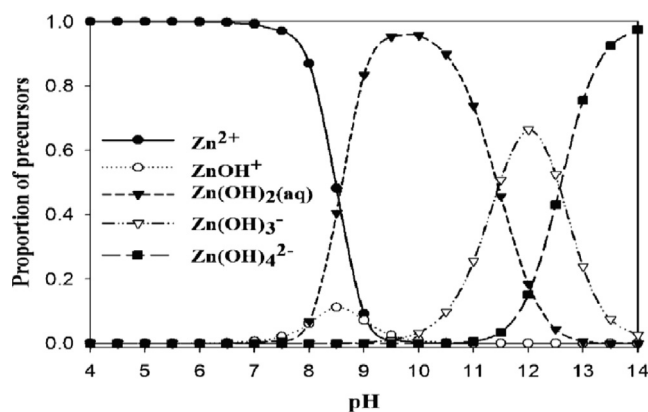


Fig. 2 Speciation diagram of Zn^{2+} species at different solution pH. The diagram is reproduced under permission from the Royal Society of Chemistry (Choi et al., 2013).

3.2. Kinetics of formation of $[\text{ZnTMPyP}]^{4+}$ complex

The kinetics of the formation of $[\text{ZnTMPyP}]^{4+}$ complex in aqueous medium at 25 ± 1 °C in $I = 0.10$ M NaNO_3 was studied spectrophotometrically by monitoring the decrease of absorbance of the free base porphyrin, $[\text{H}_2\text{TMPyP}]^{4+}$, at $\lambda_{\text{max}} = 422$ nm with time. Fig. 1 shows the spectral pattern of formation of the $[\text{ZnTMPyP}]^{4+}$ complex with time. The observed rate constants (k_{obs}) for the reactions between $[\text{H}_2\text{TMPyP}]^{4+}$ and Zn^{2+} ion at various solution pH were determined by plotting $\ln(A_t - A_\infty)$ vs time.

The rate of formation of the $[\text{ZnTMPyP}]^{4+}$ complex is first order in porphyrin that followed by the equation:

$$-d([\text{H}_2\text{TMPyP}]^{4+})/dt = k_{\text{obs}}([\text{H}_2\text{TMPyP}]^{4+}) = k_f[\text{Zn}^{2+}][[\text{H}_2\text{TMPyP}]^{4+}] \quad (5)$$

where k_{obs} is the observed first-order rate constant and k_f is the second order formation rate constant.

In order to investigate the reactivity of different Zn^{2+} -species under the present experimental conditions, the observed rate constants (k_{obs}) were measured at various solution pH. The rate constants (k_{obs}) are plotted as a function of the solution pH as shown in Fig. 3. Results show that the observed rate constant increases with increasing the solution pH and goes to its maximum value at pH = 10.30 and then slows down with further increase the pH. As seen from the Fig. 3, the increasing trend of the rate constant is very slow until the solution pH is reached at 7.44 and then increases sharply with pH. From this observation, it is concluded that the reacting species of the Zn^{2+} ion is hexaaqua Zn^{2+} , $[\text{Zn}(\text{H}_2\text{O})_6]^{2+}$ written as $\text{Zn}_{(\text{aq})}^{2+}$, at low pH which is one of the less reactive among the $[\text{Zn}(\text{H}_2\text{O})_{6-n}(\text{OH})_n]^{2-n}$ [$n = 1, \dots, 6$] species. At pH ~ 8.0, the main Zn^{2+} species is $\text{Zn}_{(\text{aq})}^{2+}$ and changes to aqua-monohydroxo, $[\text{Zn}(\text{H}_2\text{O})_5(\text{OH})]^+$, aqua-dihydroxo, $[\text{Zn}(\text{H}_2\text{O})_4(\text{OH})_2]$, aqua-trihydroxo, $[\text{Zn}(\text{H}_2\text{O})_3(\text{OH})_3]^-$, and aqua-tetrahydroxo, $[\text{Zn}(\text{H}_2\text{O})_2(\text{OH})_4]^{2-}$, species with increasing the solution pH as mentioned in equations 1–4 (Gallios and Vaclavikova, 2008; Choi et al., 2013).

As mentioned above, Zn^{2+} ion predominantly exists as its hexaaqua, $[\text{Zn}(\text{H}_2\text{O})_6]^{2+}$, species within a pH range from 4.0 to 7.44 (Fig. 2), and showed the lowest reactivity in incorpora-

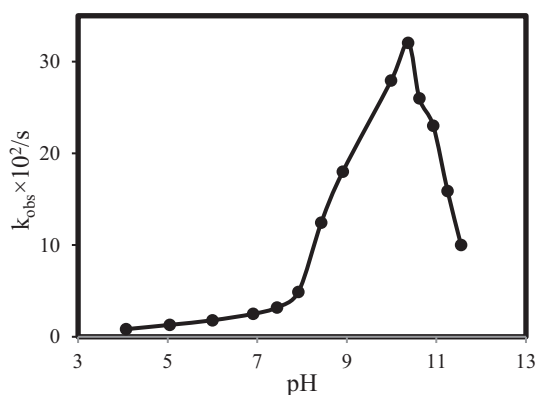


Fig. 3 Dependence of the observed rate constant, k_{obs} , as a function of solution pH ranging from 4.07 to 11.55 in $I = 0.10$ M (NaNO_3) at 25 ± 1 °C. $[\text{Zn}^{2+}] = 2.50 \times 10^{-3}$ M; $[\text{H}_2\text{TMPyP}]^{4+} = 1.24 \times 10^{-5}$ M.

tion into the free base porphyrin, $[\text{H}_2\text{TMPyP}]^{4+}$ (Fig. 3). However, the reactivity of the Zn^{2+} ion towards $[\text{H}_2\text{TMPyP}]^{4+}$ increases slightly as the presence of aqua-monohydroxo Zn^{2+} , $\text{Zn}(\text{OH})_{(\text{aq})}^+$, species increases (Fig. 3). According to the speciation diagram, the $\text{Zn}(\text{OH})_{(\text{aq})}^+$ species is distributed with the aqua-dihydroxo Zn^{2+} , $[\text{Zn}(\text{H}_2\text{O})_4(\text{OH})_2]$ simplified as $\text{Zn}(\text{OH})_{2(\text{aq})}$, at solution pH 8.5 (Fig. 2). It has been reported that the reactivity of the $\text{Zn}(\text{OH})_{(\text{aq})}^+$ species supposed to be higher than that of $\text{Zn}(\text{OH})_{2(\text{aq})}$ species (Thompson and Krishnamurthy, 1979; Sutter and Hambricht, 1993), however, the overall distribution of the aqua-monohydroxo Zn^{2+} , $\text{Zn}(\text{OH})_{(\text{aq})}^+$, species in the studied pH range is significantly low (Fig. 2). The low distribution of the $\text{Zn}(\text{OH})_{(\text{aq})}^+$ species at pH 8.5 is responsible for the poorer reactivity compared to that of $\text{Zn}(\text{OH})_{2(\text{aq})}$ species towards the $\text{H}_2\text{TMPyP}^{4+}$ (Fig. 3). On the other hand, distribution of the aqua-dihydroxo Zn^{2+} , $\text{Zn}(\text{OH})_{2(\text{aq})}$, species is extremely high within a pH range from 9.0 to 11.0 and its maximum value is observed at pH ~ 10.30 (Fig. 2). Accordingly, the $\text{Zn}(\text{OH})_{2(\text{aq})}$ species exhibits the highest reactivity among the $[\text{Zn}(\text{H}_2\text{O})_{6-n}(\text{OH})_n]^{n-2}$ species, towards $\text{H}_2\text{TMPyP}^{4+}$ at solution pH ~ 10.30 (Fig. 3). With further increase the solution pH, the trihydroxo Zn^{2+} , $\text{Zn}(\text{OH})_3^-$, species becomes the main species and eventually its reactivity goes more slow down towards the free base porphyrin, $\text{H}_2\text{TMPyP}^{4+}$, however, the negatively charged $\text{Zn}(\text{OH})_3^-$ species is supposed to be easy approached to the tetra-cationic $\text{H}_2\text{TMPyP}^{4+}$ from electrostatic force of attraction point of view. This is because the $\text{Zn}(\text{OH})_3^-$ species phases out from the aqueous system due to its low solubility, thereby resulting in the presence of its little amount in aqueous phase (Choi et al., 2013). Moreover, the extremely low concentration of the $\text{Zn}(\text{OH})_3^-$ along with the $\text{Zn}(\text{OH})_4^{2-}$ species at pH ~ 11.0 is also responsible for their less and/or least reactivity towards the free base porphyrin, $\text{H}_2\text{TMPyP}^{4+}$ (Figs. 2 and 3).

Therefore, the rate of incorporation of Zn^{2+} into the $[\text{H}_2\text{TMPyP}]^{4+}$ (for simplicity the $[\text{H}_2\text{TMPyP}]^{4+}$ written as H_2P^{4+}) is expressed by the following equations:



Due to the least reactivity of the tetrahydroxozincate(II), $\text{Zn}(\text{OH})_{4(\text{aq})}^{2-}$, species towards porphyrin and its few percent at pH = 10.30, Eq. (10) can thus be ignored, accordingly Eqs. (6)–(9) can be considered in calculating the k_{obs} .

$$\text{Therefore, } k_{\text{obs}} = k_1[\text{Zn}_{(\text{aq})}^{2+}] + k_2[\text{Zn}(\text{OH})_{(\text{aq})}^+] + k_3[\text{Zn}(\text{OH})_{2(\text{aq})}] + k_4[\text{Zn}(\text{OH})_{3(\text{aq})}^-] \quad (11)$$

According to the speciation equilibria (eqs. 1–4) and pH dependent observed rate constants, k_{obs} , (Fig. 3), the individual rate constant in Eq. (11) was calculated by averaging the observed rate constants. These are as follows: $k_1 = (0.20 \pm 0.10) \times 10^{-1}$; $k_2 = (0.70 \pm 0.50) \times 10^{-1}$; $k_3 =$

$(2.60 \pm 0.60) \times 10^{-1}$, $k_4 = (1.20 \pm 0.40) \times 10^{-1} \text{ M}^{-1}\text{s}^{-1}$ at 25 ± 1 °C. Results show that the aqua-dihydroxo Zn^{2+} , $\text{Zn}(\text{OH})_{2(\text{aq})}$, species shows the highest reactivity among the Zn^{2+} species towards the free base porphyrin $[\text{H}_2\text{TMPyP}]^{4+}$ where $k_3 = 2.60 \pm 0.60 \times 10^{-1} \text{ M}^{-1}\text{s}^{-1}$. The enhanced reactivity of the zinc-aqua-dihydroxo, $\text{Zn}(\text{OH})_{2(\text{aq})}$, species towards $\text{H}_2\text{TMPyP}^{4+}$ is comparable to the increased rate constant of $\text{Zn}(\text{OH})_2$ with hematoporphyrin IX (Paquette and Zador, 1978). The reactivity of the Zn^{2+} ion with hematoporphyrin IX decreases with increasing number of the OH^- group coordinated to the Zn^{2+} ion and found the following sequence: $k_{\text{Zn}(\text{OH})_2}^- > k_{\text{Zn}(\text{OH})_3}^- > k_{\text{Zn}(\text{OH})_4}^-$ (Paquette and Zador, 1978). Cabbiness and Marguerin (1970) also reported that the trihydroxocupriate(II), $[\text{Cu}(\text{OH})_3]^-$, species shows higher reactivity than the tetrahydroxocupriate(II), $[\text{Cu}(\text{OH})_4]^{2-}$, with the hematoporphyrin IX, *i.e.*, $k_{\text{Cu}(\text{OH})_3}^- > k_{\text{Cu}(\text{OH})_4}^{2-}$. In other reports, it has been explained that the $[\text{ZnOH}]^+$ species showed enhanced reactivity towards non-*N*-substituted porphyrins compared to that of Zn^{2+} ion where $k_{\text{ZnOH}}^+ > k_{\text{Zn}}^{2+}$ (Hambricht and Chock, 1974; Paquette and Zador, 1978; Thompson and Krishnamurthy, 1979; Sutter and Hambricht, 1993). The increased rate constants have been ascribed to the formation of hydrogen bonding between the active oxygen of the hydroxyl ligand and the pyrrolic hydrogen atom of the free base porphyrin. Tabata and Ishimi (1997) found enhanced reactivity for the ZnOH^+ species with the *N-p*-nitrobenzyl-5,10,15,20-tetrakis(4-sulfonatophenyl)-porphyrin. The better reactivity has also been elucidated due to the formation of hydrogen bonding between the oxygen atom of the hydroxo-ligand and the pyrrolic hydrogen atom of the porphyrin ring. In our previous study, we also found the enhanced reactivity of monohydroxotrichloroaurate(III), $\text{AuCl}_3(\text{OH})^-$, species towards the $[\text{H}_2\text{TMPyP}]^{4+}$ where $k_{\text{AuCl}_3(\text{OH})}^- > k_{\text{AuCl}_4}^- > k_{\text{AuCl}_2(\text{OH})_2}^- > k_{\text{AuCl}(\text{OH})_3}^-$ (Habib et al., 2004). In another investigation, monohydroxocopper (II), $[\text{Cu}(\text{OH})]^+$, species shows much more reactivity with $[\text{H}_2\text{TMPyP}]^{4+}$ compared to its aqua ion, $\text{Cu}^{2+}_{(\text{aq})}$, *i.e.*, $k_{\text{Cu}(\text{OH})}^+ \gg k_{\text{Cu}(\text{aq})}^{2+}$ (Schneider, 1975). The marked reactivities of the oxygen containing copper species also indicated the formation of hydrogen bonding between the oxygen atom of the hydroxo-ligand of monohydroxocopper(II) and the pyrrolic hydrogen of the $[\text{H}_2\text{TMPyP}]^{4+}$. Consequently, the formation of hydrogen bonding between the oxygen atom of OH^- group and the pyrrolic hydrogen atom facilitates an easy approach of the Zn^{2+} species to the porphyrin core, thereby resulting in obtaining the higher reactivity of the Zn^{2+} ion. On the contrary, the aqua- Zn^{2+} , $\text{Zn}^{2+}_{(\text{aq})}$, species is lack of hydroxo (OH^-) ligands thus might have less approaching ability to the porphyrin core that is responsible of its least reactivity towards the $\text{H}_2\text{TMPyP}^{4+}$ and found the lowest value of the rate constant: $k_1 = 0.20 \pm 0.10 \times 10^{-1} \text{ M}^{-1}\text{s}^{-1}$.

Therefore it is concluded that the presence of hydroxyl group, OH^- , is responsible for the enhanced reactivity of the Zn^{2+} species towards the free base porphyrin, $[\text{H}_2\text{TMPyP}]^{4+}$. This is due to the formation of hydrogen bonding between the oxygen atom of the OH^- group and the pyrrolic hydrogen atom of the porphyrin ring. The formation of hydrogen bonding facilitates an easy approach of the hydroxo-species of Zn^{2+} ion, $\text{Zn}(\text{OH})_n^{2-n}$, to the porphyrin core while aqua-species, $\text{Zn}^{2+}_{(\text{aq})}$, might have less approaching ability to the porphyrin core that is responsible of its least reactivity. The less reactivity of the trihydroxozincate(II), $\text{Zn}(\text{OH})_3^-$, species towards the

$\text{H}_2\text{TMPyP}^{4+}$ can be explained by taking the following factors into account: (i) presence of small amount of the $\text{Zn}(\text{OH})_3^-$ species at $\text{pH} \sim 11.25$ due to its poor solubility in aqueous medium (Choi et al., 2013) and (ii) slower displacement of the second OH^- ligand (Habib et al., 2004). The trihydroxozincate(II), $\text{Zn}(\text{OH})_3^-$, species is anionic while the free base porphyrin is tetracationic, accordingly an electrostatic force of attraction will be developed between the oppositely charged species. Such easy approach should enhance the reactivity of the $\text{Zn}(\text{OH})_3^-$ species towards the cationic $\text{H}_2\text{TMPyP}^{4+}$, however, the low concentration of the $\text{Zn}(\text{OH})_3^-$ species and slower displacement of the bound second OH^- ligand causes its less reactivity with the $\text{H}_2\text{TMPyP}^{4+}$ although the first OH^- ligand is responsible for the hydrogen bonding with the pyrrolic hydrogen.

3.3. Effect of Zn^{2+} concentration on the observed rate constants (k_{obs})

Attempts have also been taken to study the rate of reaction of formation of ZnTMPyP^{4+} as a function of concentration of Zn^{2+} at $\text{pH} = 10.30$. The observed rate constant (k_{obs}) was obtained by plotting the $\ln(A_t - A_\infty)$ vs time. The obtained values of the observed rate constants (k_{obs}) as a function of concentration of Zn^{2+} are shown in Fig. 4. The dependence of the rate on the concentration of Zn^{2+} (as shown in Fig. 4) being linear ($r^2 = 0.997$) with a small intercept almost at the origin shows that the reaction is first order with respect to both the concentrations of Zn^{2+} and porphyrin.

The formation rate constant (k_f) for $[\text{Zn}(\text{OH})_{2(\text{aq})}]/[\text{H}_2\text{TMPyP}]^{4+}$ was found to be $1.265 \times 10^{-1} \text{ M}^{-1}\text{s}^{-1}$ at $I = 0.10 \text{ M}$, NaNO_3 (25 ± 1 °C). However, Turay and Hambricht (1980) studied the kinetics of Co^{2+} and Ni^{2+} with the $[\text{H}_2\text{TMPyP}]^{4+}$ and they reported the rate constants were to be 1.10×10^{-3} and $2.10 \times 10^{-6} \text{ M}^{-1}\text{s}^{-1}$ respectively in $I = 0.50 \text{ M}$ (NaNO_3) (25 °C). A slow reaction would be expected for Zn^{2+} species, but the rate constant of $[\text{Zn}(\text{OH})_{2(\text{aq})}]$ seems to be relatively large due to the formation of hydrogen bonding between the oxygen atom of the $\text{Zn}(\text{OH})_{2(\text{aq})}$ species and the pyrrolic hydrogen atom of the porphyrin ring. Moreover, Habib et al. (2004) reported high value of the formation rate constant for the reaction between $[\text{AuCl}_3(\text{OH})]^-$ and $[\text{H}_2\text{TMPyP}]^{4+}$ was to be $3.83 \times 10^{-1} \text{ M}^{-1}\text{s}^{-1}$ for $I = 0.10 \text{ M}$ (NaNO_3) at 25 °C while Au^{3+} (d^8) ion seems

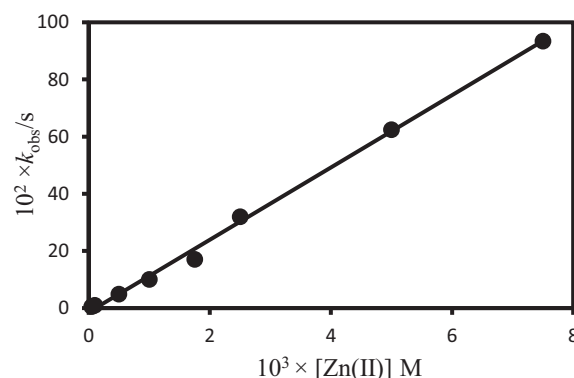


Fig. 4 Plot of the observed rate constants (k_{obs}) for the reaction of $[\text{H}_2\text{TMPyP}]^{4+}$ as a function of concentrations of Zn^{2+} in $I = 0.10 \text{ M}$ (NaNO_3) at 25 ± 1 °C. $[\text{H}_2\text{TMPyP}]^{4+} = 1.24 \times 10^{-5} \text{ M}$; $\text{pH} = 10.30$.

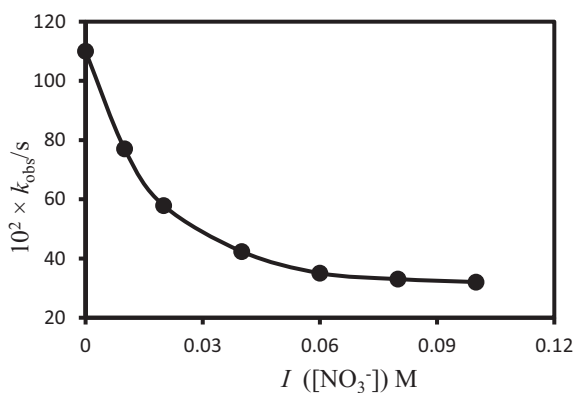


Fig. 5 Effect of ionic strength on the observed rate constant, (k_{obs}), at solution pH 10.30. $[\text{H}_2\text{TMPyP}]^{4+} = 1.24 \times 10^{-5}$ M; $[\text{Zn}^{2+}] = 2.50 \times 10^{-3}$ M; Temperature: 25 ± 1 °C.

kinetically inert (Pearson, 1963). The high reactivity of the $[\text{AuCl}_3(\text{OH})]^-$ species for the cationic porphyrin, $[\text{H}_2\text{TMPyP}]^{4+}$, is due to the negative charge and hydrogen bonding effects of the $[\text{AuCl}_3(\text{OH})]^-$ species.

3.4. Effect of ionic strength on the observed rate constants (k_{obs})

The effect of ionic strength on the reaction rate was investigated by carrying out the reaction of formation of the $[\text{ZnTMPyP}]^{4+}$ complex within a range from 0 to 10.0×10^{-2} M NaNO_3 under the same experimental conditions at solution pH 10.30. The observed rate constant (k_{obs}) was obtained by plotting the $\ln(A_1 - A_2)$ vs time at different ionic strengths. The decrease of the observed rate constants (k_{obs}) with ionic strength (Fig. 5) indicates that the Zn^{2+} species are negative that reduces the activity of the reactive species, thus resulting in slower the reaction rate.

Hambright (2002) has also investigated the variation of the rate constants of the incorporation of Zn^{2+} into $[\text{H}_2\text{TMPyP}]^{4+}$ with ionic strengths. By using the Bronsted-Bjerrum equation, the apparent net charge of the $[\text{H}_2\text{TMPyP}]^{4+}$ was found to be + 1.4. Since the direct reaction of Zn^{2+} with $[\text{H}_2\text{TMPyP}]^{4+}$ seems to be difficult, so nitrate ions reduce the repulsive force between Zn^{2+} and $[\text{H}_2\text{TMPyP}]^{4+}$ by interacting with the positively charged porphyrin tetracation, forming cation-anion aggregates of lower positive charge. Therefore, the apparent charge of $[\text{H}_2\text{TMPyP}]^{4+}$ may be much lower than the actual charge of the $[\text{H}_2\text{TMPyP}]^{4+}$ ion in the course of the reaction with Zn^{2+} compared to that of $[\text{Zn}(\text{OH})_2(\text{aq})]$. According to the Fuoss equation, the effect of ionic strength on the observed reaction rate constants divulged that the net charge on the porphyrin periphery is calculated to be + 3.4.

4. Conclusion

The present study involves: (i) speciation of Zn^{2+} in aqueous medium and (ii) kinetics and mechanism of the formation of $[\text{ZnTMPyP}]^{4+}$ complex at 25 ± 1 °C within a pH range from 4.07 to 11.55 in $I = 0.10$ M (NaNO_3). The speciation results revealed the stepwise formation of $[\text{Zn}(\text{H}_2\text{O})_{6-n}(\text{OH})_n]^{2-n}$ species at different solution pH. The aqua-dihydroxo species of the Zn^{2+} ion *i.e.*, $[\text{Zn}(\text{OH})_2(\text{aq})]$ showed the highest reactivity

towards the $[\text{H}_2\text{TMPyP}]^{4+}$ because of formation of the hydrogen bonding between the oxygen atom of the hydroxyl group of $[\text{Zn}(\text{OH})_2(\text{aq})]$ species and the pyrrolic hydrogen atom of the free-base porphyrin, $[\text{H}_2\text{TMPyP}]^{4+}$. The net charge on the porphyrin periphery was calculated to be + 3.4, and the rate of incorporation of the $[\text{Zn}(\text{OH})_2(\text{aq})]$ into $[\text{H}_2\text{TMPyP}]^{4+}$ is not too slow as expected.

Declaration of Competing Interest

The authors declare no competing financial interest.

Acknowledgement

The authors acknowledge to the Ministry of Science and Technology, the People's Republic of Bangladesh for financial support to carry out this work under the project "Photoelectrochemical splitting of water into hydrogen using solar light".

Appendix A. Supplementary material

Supplementary data to this article can be found online at <https://doi.org/10.1016/j.arabj.2020.06.011>.

References

- Anula, H.M., Myshkin, E., Guliaev, A., Luman, C., Danilov, E.O., Castellano, F.N., Bullerjahn, G.S., Rodgers, M.A.J., 2006. Photo processes on self-associated cationic porphyrins and plastocyanin complexes I. Ligation of plastocyanin tyrosine 83 onto metalloporphyrins and electron-transfer fluorescence quenching. *J. Phys. Chem. A* 110, 2545–2559.
- Baes, C.F., Mesmer, R.E., 1976. *The Hydrolysis of Cations*. Wiley, New York.
- Burgess, J., 1978. *Metal ions in Solution*. Ellis Horwood, New York, p. 147.
- Cabbiness, D.K., Margerum, D., 1970. Effect of macrocyclic structures on the rate of formation and dissociation of copper(II) complexes. *J. Am. Chem. Soc.* 92, 2151–2153.
- Choi, C.-H., Su, Y.-W., Chih-hung Chang, C.C.-H., 2013. Effects of fluid flow on the growth and assembly of ZnO nanocrystals in a continuous flow microreactor. *CrystEngComm* 15, 3326–3333.
- Funahashi, S., Ito, Y., Kakito, H., Inamo, M., Hamada, Y., Tanaka, M., 1986. Metal ion incorporation into N-methyl-5,10,15,20-tetrakis (4-sulfonatophenyl) porphine and its differential rates as applied to the kinetic determination of copper(II) and Zn(II) in serum. *Mikrochim. Acta* 88, 33–47.
- Gallios, G.P., Vaclavikova, M., 2008. Removal of chromium (VI) from water streams: a thermodynamic study. *Environ. Chem. Lett.* 6, 235–240.
- Habib, A., Tabata, M., Wu, Y., 2004. Kinetics and mechanism of gold (III) incorporation into tetrakis(1-methylpyridium-4-yl) porphyrin in aqueous solution. *J. Porphyrins Phthalocyanines* 8, 1269–1275.
- Hambright, P., Chock, P.B., 1974. Metal-porphyrin interactions. III. Dissociative-interchange mechanism for metal ion incorporation into porphyrin molecules. *J. Am. Chem. Soc.* 96, 3123–3131.
- Hambright, P., 1975. 1975. In: Smith, K.M. (Ed.), *Porphyrins and Metalloporphyrins*. Elsevier, Amsterdam, pp. 232–278.
- Hambright, P., 2002. In: *The Porphyrin Handbook*, Kadish, K.M., Guillard R. (Ed). Academic Press, vol. 3, pp. 18. 163.
- Imran, M., Ramzan, M., Qureshi, A.K., Khan, M.A., Muhammad Tariq, M., 2018. Emerging applications of porphyrins and metal-

- loporphyrins in biomedicine and diagnostic magnetic resonance imaging. *Biosensors* 8, 95.
- Kawamura, K., Igarashi, S., Otsuyanagi, T., 1988. Acceleration effect of L-tryptophan on metal ion exchange reaction of cadmium(II) with water soluble-porphyrin-lead(II) complex and its application to stopped-flow spectrophotometric determination of nM level of cadmium(II). *Anal. Sci.* 4, 175–179.
- Lavallee, D.K., 1985. Kinetics and mechanisms of metalloporphyrin reactions. *Coord. Chem. Rev.* 61, 55–96.
- Lavellee, D.K., 1987. *The Chemistry and Biochemistry of N-Substituted Porphyrins*. VCH Publishers, New York.
- Longo, F.R., Brown, E.M., Rau, W.G., Adler, A.D., 1979. In: *Kinetic and Mechanistic Studies of Metalloporphyrin Formation in the Porphyrins*, Dolphin, D. (Ed). vol. V, Academic Press, New York, 459–481.
- Makino, T., Itoh, J.I., 1981. A highly sensitive colorimetric determination of serum copper using α , β , γ , δ -tetrakis(4-N-trimethylaminophenyl)-porphine. *Clin. Chim. Acta* 111, 1–8.
- Margerum, D.W., Cayley, G.R., 1978. In: *Coordination Chemistry*. American Chemical Society, Washington, DC, pp. 1–194.
- Nyarko, E., Hara, T., Grab, D.J., Habib, A., Kim, Y., Nikolskaia, O., Fukuma, T., Tabata, M., 2004a. In vitro toxicity of palladium(II) and gold(III) porphyrins and their aqueous metal ion counterparts on *Trypanosoma brucei brucei* growth. *Chemico-Biological Inter.* 148, 19–25.
- Nyarko, E., Hanada, N., Habib, A., M. Tabata, M., 2004b. Fluorescence and phosphorescence spectra of Au(III), Pt(II) and Pd(II) porphyrins with DNA at room temperature. *Inorganica Chim. Acta* 357, 739–745.
- Paquette, G., Zador, M., 1978. Kinetics of interaction of Zn(II) with hematoporphyrin IX in basic aqueous solution. *Inorg. Chim. Acta* 26, L23–L24.
- Pearson, R.G., 1963. Hard and soft acids and bases. *J. Am. Chem. Soc.* 85, 3533–3539.
- Ptaszynska, A.A., Trytek, M., Borsuk, G., Buczek, K., Rybicka-Jasinska, K., Gryko, D., 2018. Porphyrins inactivate *Nosema* spp. microsporidia. *Sci. Rep.* 8, 5523.
- Rapozi, V., Zorzet, S., Zacchigna, M., Pietra, E.D., Cogoi, S., Xodo, L.E., 2014. Anticancer activity of cationic porphyrins in melanoma tumour-bearing mice and mechanistic *in vitro* studies. *Mol. Cancer* 13, 75–91.
- Roohani, N., Hurrell, R., Kelishadi, R., Schulin, R., 2013. Zinc and its importance for human health: An integrative review. *J. Res. Med. Sci.* 18, 144–157.
- Schneider, W., 1975. *Struct. Bonding (Berlin)* 23, 123–166.
- Shamim, A., Hambright, P., 1980. Exchange reactions of transition metal ions and labile cadmium porphyrins. *J. Inorg. Nucl. Chem.* 42, 1645–1647.
- Sutter, T.P.G., Hambright, P., 1993. The effects of peripheral substituents of the kinetics of zinc ion incorporation and acid catalyzed removal from water soluble sulfonatedporphyrins. *J. Coord. Chem.* 30, 317–326.
- Tabata, M., Tanaka, M., 1983. Kinetics and mechanism of cadmium (II) ion assisted incorporation of manganese(II) into 5,10,15,20-tetrakis(4sulphonatophenyl)porphyrinate(4-). *J. Chem. Soc. Dalton Trans.*, 1955–1959
- Tabata, M., Tanaka, M., 1991. Porphyrins as reagents for trace-metal analysis. *Trends Anal. Chem.* 10 (1991), 128–133.
- Tabata, M., Ishimi, H., 1997. Kinetics and mechanism for the formation and dissociation reactions of 21-(4-nitrobenzyl)-5,10,15,20-tetrakis(4-sulfonatophenyl)-23*H*-porphyrinatoZn(II) and -cadmium(II). *Bull. Chem. Soc. Jpn.* 70, 1353–1359.
- Tanaka, M., 1983. Kinetics of metalloporphyrin formation with particular reference to the metal ion assisted mechanism. *Pure Appl. Chem.* 55, 151–158.
- Thompson, A.N., Krishnamurthy, M., 1979. Peripheral charge effects on the kinetics of Zn(II)-porphyrin system. *J. Inorg. Nuclear. Chem.* 41, 1251–1255.
- Tsolekile, N., Nelana, S., Oluwafemi, O.S., 2019. Porphyrin as diagnostic and therapeutic agent. *Molecules* 24, 2669.
- Turay, J., P. Hambright, P., 1980. Activation parameters and a mechanism for metal-porphyrin formation reactions. *Inorg. Chem.* 19, 562–564.
- Varchi, G., Foglietta, F., Canaparo, R., Ballestri, M., Arena, F., Sotgiu, G., Fanti, S., 2015. Engineered porphyrin loaded core-shell nanoparticles for selective sonodynamic anticancer treatment. *Nanomedicine* 10, 3483–3494.